Overview of the status of radiative transfer models for satellite data assimilation

Jérôme Vidot

Centre de Météorologie Spatiale
Météo-France, Lannion, France

ABSTRACT

This paper provides an overview of the status of radiative transfer models for satellite data assimilation. The radiative transfer model for satellite data assimilation also known as the satellite radiance operator is one of the most complex and the most computationally expensive operators in the overall cost of assimilation. Therefore weather forecast centres require fast radiative transfer models to assimilate the huge amount of observations from various satellites and sustainable for operational purposes. The assimilation of satellite radiance is currently operated in all-sky conditions in the microwave and in clear-sky and overcast cloudy conditions in the infrared. To make this possible, these radiative transfer models are based on fast atmospheric transmittance models as well as on cloud scattering approximation. The modelization, the validation and the future developments of the two main radiative transfer models RTTOV and CRTM are described here.

1 Introduction

In the beginning of the 1990's, when the assimilation of TIROS Operational Vertical Sounder (TOVS) top-of-atmosphere (TOA) radiances began operational in the European Centre for Medium Weather Forecast (ECMWF) numerical weather prediction (NWP) model, the accurate modelization of atmospheric radiative transfer started to be of central importance in the satellite data assimilation for NWP community. In theory, atmospheric radiative transfer is the physical phenomenon of energy transfer in the form of electromagnetic radiation. It describes the propagation of radiation through the Earth's atmosphere affected by interaction processes between radiation and atmospheric constituents (gas, clouds and aerosols) and surface. The purpose of atmospheric radiative transfer is to solve the radiative transfer equation (RTE) that describes these interaction processes in a mathematical way and to develop numerical radiative transfer models (RTM).

For the assimilation of satellite observations in NWP, dedicated RTM have been developed to link atmospheric variables of NWP models to satellite observations during the assimilation process since satellites do not measure directly temperature, moisture or cloud properties. Those RTM must be fast in order to assimilate the huge amount of satellite radiances. They must be sustainable in operational environment and accurate, at least below the instrument noises in clear-sky condition. They are often called fast RTM or satellite radiance operators. There are two main fast RTM now in use as satellite radiance operators. The first one is the Community Radiative Transfer Model (CRTM, see http://www.star.nesdis.noaa.gov/smcd/spb/CRTM/) which have a long scientific heritage beginning in mid 1970's with the work of Larry M. McMillin and Henry E. Fleming but started to be sustainable in 2005 by NOAA and is currently operational at NCEP. The second one is the radiative transfer model for TOVS (RTTOV, see https://nwpsaf.eu/deliverables/rtm/) which have been firstly coded in the beginning of the 1990's by John Eyre and now is supported by the NWP Satellite Application Facilities (SAF). RTTOV is currently operational at ECMWF, UK Met-Office, Météo-France, Japan

Meteorological Agency (JMA), Deutscher WetterDienst (DWD), China Meteorological Administration (CMA) and many other national weather services. CRTM and RTTOV developers share ideas, improvements and developments through the Radiative Transfer and Surface Properties(RTSP) sub group of the International TOVS Working Group (ITWG). See for more information https://groups.ssec.wisc.edu/groups/itwg/rtsp.

Fast RTM for satellite data assimilation have many distinctive features compared with classical RTM. They must provide fast simulations of many satellite instruments from passive infrared (IR) sounders and imagers (between 3 and 20 μm or 500 and 3000 cm^{-1}) to passive microwave (MW) sounders (between 10-200 GHz). As an example, there are more than 50 instruments currently assimilated in the Integrated Forecast System (IFS) with RTTOV. Satellite radiance operators are requested to provide mandatory information for the assimilation process. These information are the forward model, i.e. the simulated TOA radiances or brightness temperature (BT), and the tangent linear, the adjoint and the jacobian models. The major constraint of satellite radiance operators are their entries, which are not optical properties of atmospheric constituents but NWP model variables (i.e., profiles of temperature, pressure, moisture, cloud water content, etc…). The n satellite radiance operator make use of many parameterizations to relate these NWP model variables to optical properties. These parameterizations are often linear in order to facilitate derivative calculations. For operational purposes, satellite radiance operator – or fast RTM – must modelize many physical interactions between radiation and atmospheric constituents such as gaseous absorption, cloud scattering and overlapping and land and ocean surface emissivities. They must also consider instrument-specific effects such as the Zeeman effect, the CO_2 pressure cell variation and the postlaunch calibration modification or physical effects that are considered in operational environment such as non-local thermodynamic equilibrium (NLTE) and solar contribution. All these aspects will be described in this paper.

2 Atmospheric radiative transfer physical principles

There are three physical interactions when an incident radiation hit a particle in the atmosphere: (1) the absorption of the radiation by the particle which corresponds to an attenuation of the incident radiation by energetic modification (internal heating or chemical reaction); (2) the emission of radiation by the particle at the same wavelength as the incident radiation which corresponds to an isotropic radiation increase by molecular excitation due to absorption (according to Kirchhoff's Law); (3) the scattering of the radiation by the particle which corresponds to an attenuation of the incident radiation by deviation in other directions than the original radiation trajectory. Finally, the total extinction is given by the sum of absorption and scattering. Absorption, scattering and extinction are represented by coefficients *k* (units of inverse length) that depend on the particle's microphysical and optical properties (refractive index, size distribution and shape).

2.1 General form of RTE and source function components

In order to provide the general form of the radiative transfer equation (RTE) that is currently uses by fast RTM, many hypothesis have to be assumed. The Earth atmosphere is considered as a stratified piling of many homogenous and plane-parallel layers where local thermodynamic equilibrium (LTE) applied and where 3D effects (i.e., horizontal transport of photons) and polarization are ignored.

The differential change of monochromatic radiance dR (at wavenumber v) along the path ds within an atmospheric layer of thickness dz in the direction given by spherical coordinates (θ, ϕ) is given by:

$$\mu \frac{dR(\nu; \mu, \phi)}{dz} = -k_e(\nu)R(\nu; \mu, \phi) + k_e(\nu)J(\nu; \mu, \phi) \tag{1}$$

where $\mu = \cos(\theta)$, $k_e(\nu)$ is the spectrally-dependent extinction coefficient of the homogeneous atmospheric layer, R is the incident radiance and J is the source function. The first term of the righthand side of Eq. (1) is negative due to an attenuation of radiation by extinction, whereas the second term of the right hand side of Eq. (1) is positive due to an increase of radiation provided by the source function. The source function have two components: emission and scattering.

2.2 Source function components

The emission component of the source function J is due to thermal emission from the sun and from the terrestrial environment. The radiance emitted by an object considered as a blackbody is given by the Planck's function B which depends on the temperature and on the wavelength. The Figure 1 represents the normalized (i.e., the areas under each curve are equal) blackbody emission curves for three temperatures (the sun at 6000 K and the terrestrial environment at 300 K and 250 K).
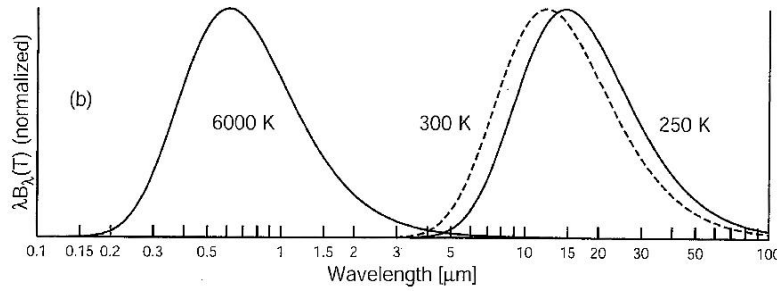

Figure 1: Normalized blackbody emission curves at temperatures typical of the sun andof the earth and atmosphere (from Figure 6.2 page 118 of Petty, 2006).

The blackbody emission from the sun have a maximum in the visible range whereas blackbody emissions from the terrestrial environment have maximums in the infrared domain. Figure 1 shows that for most satellite applications, the source function coming from the sun and from the terrestrial radiation can be treated separately.

The scattering component of the source function J depends also on the spectral domains but also on the particle size. The significance of its effect is given by the size parameter x:

$$x = \frac{2\pi r}{\lambda}$$

where λ is the wavelength and r is the particle size. Figure 2 shows the scattering regime for main atmospheric particle types and for different spectral domains. In the IR region, scattering from molecules is negligible whereas in the MW region, scattering from both molecules and aerosols is negligible. The theoretical treatment of scattering (through Rayleigh, Mie or geometric optics theories) depends on the size parameter.
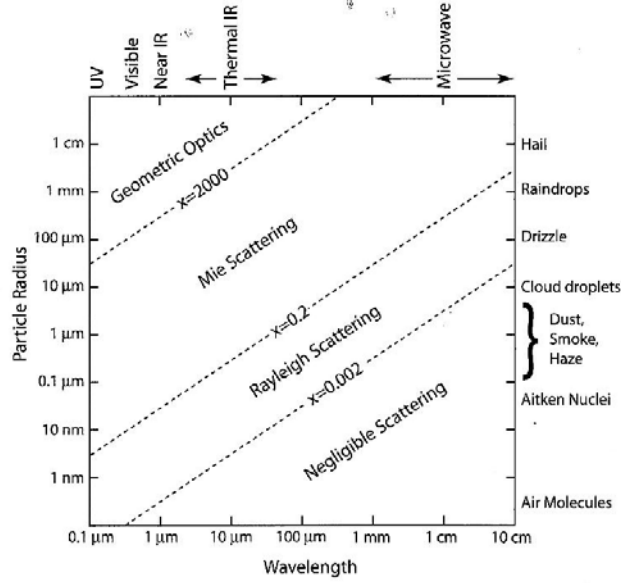
Figure 2: Relationship between particle size, radiation wavelength and scattering behaviour for atmospheric particles. Diagonal dashed lines represent rough boundaries between scattering regimes (Figure 12.1 page 346 of Petty, 2006).

3 Satellite radiance operators

3.1 Clear-Sky RTE

The clear-sky infrared and microwave RTE is based on the Schwarzschild's equation when considering an homogeneous plane-parallel nonscattering atmosphere. In that case, molecular absorption is only considered and the source function *J* is given by atmospheric emission (no solar contribution are involved). The Schwarzschild's equation is given from Eq. (1) as:

$$\mu \frac{dR(\mu)}{dz} = -k_a R(\mu) + k_a B(T)$$

(2)

Where k_a is the spectrally-dependent absorption coefficient of the atmospheric layer and $B(T)$ is the Planck function of the atmospheric layer of temperature *T*. In Eq. (2) and hereafter, the spectral dependence is omitted for clarity. The azimuth-independence applies due to the isotropic characteristic of emission. The solution of the Schwarzschild's equation provide the clear-sky TOA radiance R_{clr} as observed by an IR or MW instrument over a specular reflecting surface:

$$R_{clr}(\mu) = t_{tot}(\mu)\varepsilon_{sfc}(\mu)B(T_{sfc}) + \int_{t_{tot}}^{1} B(T)dt + [1 - \varepsilon_{sfc}(\mu)]t_{tot}^2(\mu) \int_{t_{tot}}^{1} \frac{B(T)}{t^2}dt$$

(3)

The first term of the right hand side of Eq. (3) is due to surface emission attenuated by the total atmospheric transmittance from TOA to surface t_{tot}. This term involves the radiance emitted by the surface as the product of the surface emissivity ε_{sfc} and the blackbody emission at surface temperature T_{sfc}. The second term of the right hand side of Eq. (3) is due to upwelling atmospheric emission and the third term of the right hand side of Eq. (3) is due to downwelling atmospheric emission specularly reflected by the surface.

To simulate satellite observation, we must consider that passive IR/MW instrument's channels are polychromatic and not monochromatic. Ideally, we would solve the RTE at many wavenumbers and integrate the resulting radiances over the channel spectral response function (SRF). In practice, we integrate atmospheric transmittances over the SRF and solve the RTE once per channels.

3.2 Atmospheric transmittance

The principal unknown of Eq. (3) is the atmospheric transmittance t. Transmittance express the attenuation by molecules of the incident radiation by an atmospheric layer in the direction μ and is given by:

$$t(\mu) = e^{(-\tau_a/\mu)}$$

(4)

where τ_a is the absorption optical depth of the atmospheric layer given by the integration of the absorption coefficient between altitudes z_1 and z_2, namely:

$$\tau_a = \int_{z_1}^{z_2} k_a dz$$

(5)

The absorption coefficient is written as:

$$k_a(\nu) = \sum_{i=1}^{M} N_i \sigma_{a,i}(\nu) = \sum_{i=1}^{M} N_i [\sigma_{cont,i}(\nu) + \sum_{j=1}^{L_i} S_{ij} f_{ij}(\nu - \nu_{ij}, P, T)]$$

(6)

where N is the number density of atmospheric absorber i, M is the total number of different molecular species present in the layer and σ_a their absorption cross sections. Absorption cross section has two components, one from the continuum σ_{cont} and one from absorption lines. In Eq. (6), S is the absorption line strength, f is the absorption line shape simulated with a certain function (i.e., Voigt) and L is the number of significant absorption lines. The line's number, position and strength are provided by spectroscopic database (i.e., from HITRAN (Rothman et al., 2009) or GEISA (Jacquinet-Husson et al., 2008)) and σ_{cont} is given by a certain formulation (i.e., the MT_CKD (Mlawer et al., 2012) model for H_2O). Transmittances are calculated by Line-by-line (LBL) models (i.e., LBLRTM,GENLN2, AMSUTRAN,…) by assuming atmospheric profile s of N_i.

3.3 Fast atmospheric transmittance model

Transmittances from LBL models are very accurate but must be simulated at very low spectral intervals (typically 0.001 cm^{-1} for IR hyperspectral sounders) to reproduce fine absorption features. In operational context, these simulations are too computationally expensive. To speed up the calculation, fast atmospheric transmittance methods were developed in the mid 1970's by McMillin and Fleming (1976). The principal idea of these fast models is to perform a multivariate Taylor expansion of the formulation of the transmittance ratio between two adjacent layers (often called effective transmittance). Then, the absorption optical depth in a channel i from TOA to level j can be predicted as:

$$\tau_{a,i,j} = \tau_{a,i,j-1} + \sum_{k=1}^{K} c_{i,j,k} X_{i,k}$$

(7)

where c are the coefficients and X the predictors (with total K values). Predictors are functions of atmospheric variables (pressure, temperature, absorber amount) and secant (inverse cosine of zenithal angle). Coefficients are precalculated from a training dataset of atmospheric profiles that must represent the natural variability of the Earth's atmosphere. Two approaches for the vertical coordinates can be used, either at fixed pressure levels (McMillin and Fleming, 1976) or at fixed absorber levels (McMillin et al., 1979).

For CRTM, both approaches can be used, called at present time the optical depth in pressure space (ODPS, Chen et al., 2010) method and the optical depth in absorber space (ODAS) method which is an improvement of the OPTRAN version 6 model (McMillin et al., 2006). The CRTM training dataset is composed of 48 UMBC atmospheric profiles (Strow et al., 2003) interpolated at 101 levels.

For RTTOV, an improved fixed pressure levels method is currently used (Eyre, 1991; Saunders et al.,1999; Matricardi et al., 2004) with a training dataset of 83 ECMWF 91 levels profiles selected from the work of Chevallier et al. (2006) and interpolated at 101 levels. Coefficients are provided at either 101 levels or at 51 levels for RTTOV version 10 and at 54 levels for RTTOV version 11 with fixed minimum and maximum values, i.e. 0.005 and 1100 hPa, respectively.

3.3.1 Predictors selection

The number of predictors depends on the absorber. In fast RTMs, we separate atmospheric molecules in two types of absorbers. Some of them are considered as uniformly mixed in the atmosphere (i.e. CFCs, N_2, O_2, etc…) and others are considered as variable in th e atmosphere (i.e. H_2O, O_3, CO_2, etc…). In earlier version of RTTOV a number of 10 p redictors were used for both uniformly-mixed gases and variable H_2O (Eyre, 1991). Nowadays, there are 3 versions of predictors. In predictors version 7 (named like that because it was implemented in RTTOV version 7), 10 predictors is used for uniformly-mixed gases, 15 for H_2O and 11 for O_3 (Saunders et al., 1999). In predictors version 8, a separation between H_2O absorption lines (with 12 predictors) and H_2O continuum (with four predictors) was introduced as well as the add of CO_2 as variable absorber with ten predictors. In predictors version 9, more variable absorbers were included (CH4, CO, and N_2O) for hyperspectral sounders and predictors were optimally selected (see Matricardi et al. (2004) for details). In CRTM, a selection of number of predictors is done over a pool of 18 predictors (McMillin et al., 2006; Chen et al., 2010).

3.3.2 Instrument-specific effects on coefficients

Some effects specific to a certain instrument can affect the calculations of coefficients. These may arise out of the instrument itself (the so-called Zeeman effect, the CO_2 cell pressure variation or due to post launch calibration modification) or may arise out of the time when the instrument were operated. The Zeeman effect is the effect of splitting a spectral line into several components in the presence of a static magnetic field. It affect typically high peaking MW channels with error up to 0.5 K for AMSU-A to 10 K for mesospheric channels of SSMIS. Fast correction model were developed for RTTOV and CRTM (Han et al., 2006). The approach uses a predictor-based optical depth correction for each channels of impacted instruments. The second instrumental effect is due to variations of in-cell pressures on the SSU Pressure Modulated Radiometer (PMR) with CO_2 gas cell.

The nominal mean pressure cell of each channel provides measurement sensitivity at very high altitude (around 1.5, 5 and 15 hPa). But, it was shown that the mean pressure cell changes after launch causing a change in the channel SRF (Kobayashi et al., 2009). Both CRTM and RTTOV have implemented a correction of the optical depth that depends on the input mean pressure cell. The last effect on coefficient is due to modification of the channel SRF after launch. This is the case for MODIS where 5 channels were found to have shifted when comparing to AIRS (Tobin et al., 2006). This was also the case for HIRS (Cao et al., 2005) and for AMSU-A (Lu and Bell, 2014). The last case where coefficients has to be adapted is when the instruments where operated many years ago. Then the training dataset has to be adjusted to reflect the state of the atmosphere at this time. This is for example the case for CO_2 and CH_4. These adapted coefficients may improved reanalysis when assimilate observations from first space instruments.

3.4 Models or atlases for surface emissivity

To simulate satellite observations with Eq. (3), surface emissivity has to be provided. Fast RTM make use of different models or atlases as first-guess values of surface emissivity. In the infrared, the surface emissivity is provided by the Infrared Surface Emissivity Model (ISEM: Sherlock, 1999) over water and by the University of Wisconsin infrared land surface emissivity atlas (UWIREMIS: Borbas and Ruston, 2010) for land surfaces including snow and sea ice surfaces. In the microwave, the surface emissivity is provided by an atlas from the Centre National de la Recherche Météorologique (CNRM: Karbou et al., 2005) or from the Tool to Estimate Land Surface Emissivities in the Microwave (TELSEM: Aires et al., 2011) for land surfaces and from the fast microwave emissivity model (FASTEM: Liu et al., 2011) for water surfaces. The UWIREMIS, CNRM and TELSEM databases were developed from satellite measurements in order to better characterize the spatial and temporal variability of natural surfaces as seen from a satellite.

3.5`Cloudy-sky RTE

3.5.1 Infrared domain

In the infrared domain, the assimilation of cloudy-sky radiances make uses of the grey cloud approximation (Eyre, 1991) where no scattering is involved. The TOA radiance in presence of cloud is written as:

$$R(\mu) = (1 - N)R_{clr}(\mu) + NR_{cld}(\mu)$$

(8)

where N is the fractional cloud cover (for single cloud layer and cloud top emissivity of 1) and R_{cld} is the overcast cloudy radiance given by:

$$R_{cld}(\mu) = t_{cld}(\mu)B(T_{cld}) + \int_{t_{cld}}^{1} B(T)dt$$

(9)

where t_{cld} is the transmittance from TOA to the top of the cloud layer and T_{cld} is the cloud temperature. This method is operational at ECMWF (McNally, 2009) where the cloud cover and cloud top pressure are retrieved by the CO_2-slicing method (Chahine, 1974). Furthermore only 100%-overcast scenes are assimilated (i.e., N=1). However, this method produce ambiguities for very thin cloud and multi-layered cloud (Pavelin et al., 2008) and low cloud are difficult to detect due to weak contrast with surface temperature.

3.5.2 Microwave domain

In the microwave domain, the scattering by clouds is introduced. In that case the source function of Eq. (1) is modified with contributions from emission and scattering from hydrometeors, as:

$$J(\mu) = (1 - \omega_0)B(T) + \frac{\omega_0}{2} \int_{-1}^{1} R(\mu)P(\mu; \mu')d\mu'$$

(10)

where *P* is the phase function that give the probability that a radiance coming from direction *μ'* is scattered in direction *μ* and ω_0 is the single scattering albedo given by:

$$\omega_0 = \frac{k_s}{k_e} = \frac{k_s}{(k_a + k_s)}$$

(11)

where k_s is the scattering coefficient. The final RTE given by Eqs. (1) and (10) cannot be solved analytically and many numerical methods exist to solve the RTE. For fast simulations, RTTOV uses the Delta-Eddington approximation method (Bauer et al., 2006) whereas CRTM has two other different solvers, the Advanced Matrix Operator Method (Liu and Weng, 2013) and the Successive Order of Interaction (Heidinger et al., 2006) methods. CRTM solvers apply also in the IR domains but are not used operationally due to prohibitive computation time.

In RTTOV, four hydrometeors are considered (liquid cloud, ice cloud, rain and snow). The Mie theory is used to calculate optical properties (single scattering albedo and extinction) but this theory assume perfect spheres. Then, new model for ice and snowflakes were implemented by Geer and Baordo (2013). This new model is based on Look-Up Tables of optical properties from the Discrete Dipole Approximation method (Liu et al., 2008) and with new particle size distribution model (Field et al.,2007). In CRTM, optical properties for six clouds types (water, ice, rain, snow, graupel and hail) are proposed (see Chen et al. (2008) for details).

3.5.3 Cloud Overlap

To efficiently take into account the NWP model variable of the cloud fraction (CF) profile, cloud overlap methods have been introduced in RTTOV. For MW, maximum CF and single cloud layer were firstly assumed (Bauer et al., 2006). But it has been shown that cloud layer with maximum CF is often not the one with the closer to reality optical depth. Then, an averaged CF and single cloud layer were implemented (Geer et al., 2009). The main result was a decrease of the RMS error by 40% in rainy areas. For IR, the maximum random overlap is used (Matricardi, 2005). It is planned to add similar methods in CRTM.

3.6 Validation

Validation of fast RTM is an important step towards the satellite data assimilation. It can be realized in different manners: against accurate LBL models for clear-sky atmospheres, against full scattering models for cloudy-sky atmospheres, with ground-based atmospheric profiles, NWP fields or aircraft measurements. All methods provide insights in the strength and weakness of fast RTM models.

3.6.1 Clear-sky

The work of Garand et al. (2001) was the first attempt to validate both TOA radiances and jacobians from LBL and fast RTM models in clear-sky conditions. This work compared 29 models for seven IR and four MW channels and for 42 atmospheric profiles. The main results were the followings. Firstly, LBL models agree to within 0.05–0.15 K. IR BTs from fast RTM are reproduced to within 0.25 K as compared with LBL models, whereas in MW BTs are better reproduced (within 0.1 K). Jacobians intercomparison were mostly found to be useful to detect some problem in out-of-limits profiles, continuity in level-to-TOA transmittances and vertical interpolation. Some issues were mentioned at the end of the study for future validation exercise. Firstly, the airmass dependence of bias was not fully studied. Secondly, intercomparison at hyperspectral resolution for IR was recommended (AIRS or IASI) to carefully evaluate ozone and water vapor spectroscopy.

Another intercomparison study was done with real satellite data by Saunders et al. (2007). A single AIRS spectra were used over a ground based station of an ARM site. In this study, 14 models were compared and 49 atmospheric profiles were used. It was founded that fast RTMs agreed to $\pm$ 0.1 K and difference with AIRS observations is typically $\pm$ 1 K (up to $\pm$ 3 K). It was also pointed out that when using real satellite measurements, highest sources of error come from input profiles and surface emissivities.

The last intercomparison was done in operational environment with IASI satellite data (Matricardi, 2009). RTTOV was compared to three LBL models (kCARTA, GENLN2 and LBLRTM) during a 12-hours 4D-Var windows (IFS cycle 33R1) between 1 and 15 April 2008. Three regions were studied (North Hemisphere, Tropics and Southern Hemisphere). Bias were founded generally within $\pm$ 1 K in all regions. In CO_2 bands, the bias is higher for one LBL model and highlight the effect of treatment of line mixing in the model. In O_3 band, bias went up to 2 K (same for all LBL) probably due to some error in the input profiles. Finally, possible systematic moist bias in ECMWF tropical field was found and was explained by higher bias in H_2O band.

3.6.2 Cloudy-sky

Cloudy-sky validation was done for RTTOV in the MW with full scattering model (Bauer et al., 2006). An ECMWF 1D+4DVar rain assimilation run with 8290 profiles was compared. Errors were found to be less than 0.5 – 1 K. Issue on the treatment of the cloud overlap was pointed out

For CRTM, both IR and MW domains were validated with collocated observations and retrievals from AMSU-A, MHS and AVHRR against CloudSat over ocean (Chen et al., 2008). In the MW, good agreement was pointed out with larger bias below 2.4 K and larger RMS below 3.9 K for AMSU-A and MHS. In the IR, bias of 2 K and standard deviation between 3 and 6K were found and those depends on the cloud type.

4 New improvements

4.1 Cloudy-Sky Infrared RTE

Scattering in the IR has been introduced in RTTOV by using the Chou scaling method (Chou et al.,1999). The total optical depth of a layer containing scatters is written as:

$$\tau_{tot} = \tau_a + b\tau_s \tag{12}$$

where τ_s is the scattering optical depth and b is the backscattering fraction (see Matricardi et al. (2005) for the formulation of b). Optical properties for 5 types of liquid cloud (2 stratus and 3 cumulus clouds) are tabulated in function of the liquid water content (LWC). For ice cloud, different parametrization of optical properties in function of ice water content are proposed. The Chou scaling method have been already been used for IR cloudy radiances assimilation studies. For examples, a new IASI channel selection for cloudy retrievals of 144 channels have been proposed by Martinet al. (2013) in extension to the current 366 channels of Collard (2007). Test of feasibility to add the cloud variables to the state vector of the assimilation system were studied by Martinet et al. (2014) and observation minus background departure analysis of all sky-IASI data were found to be less than 10K by Okamoto et al. (2013) when using IR cloud scattering from RTTOV.

4.2 Non Local Thermodynamic Equilibrium (NLTE)

In real atmosphere, LTE can break down at extremely high altitude where spontaneous emission is low and when other sources of radiation are present. This is the case in CO_2 band during daytime above 40 km where significant NLTE emission occurs. Simulations of TOA brightness temperature between NLTE and LTE show several Kelvin differences when the sun is at zenith. A fast NLTE correction method has been developed from CRTM (Chen et al., 2013) and adapted for RTTOV. The TOA radiance is corrected from the term given by:

$$\Delta R^{NLTE}(\mu, \mu_s) = c_0(\mu, \mu_s) + c_1(\mu, \mu_s)T_1 + c_2(\mu, \mu_s)T_2 \tag{13}$$

where $c_{0\text{-}2}$ are coefficients derived from statistical regression of a fit function against the training dataset of 48 UMBC profiles, T_1 is the mean temperature between 0.005 and 0.2 hPa and T_2 is the mean temperature between 0.2 and 52 hPa. The correction is applied between 2225 cm^{-1} and 24000 cm^{-1} and reproduces training data with a mean bias of 0.01K and a maximum standard deviation of 0.1 K.

4.2 Solar contribution (RTTOV only)

The Figure 1 shows that the solar contribution can be present as far as tenth of microns. In general, the solar contribution is not accounted for in operational environment. However during daytime and particularly at short-wave infrared domains, the solar contribution has to be taken into account. For that a new term in the source function of Eq. (2) has to be added. In RTTOV, the solar contribution is calculated as:

$$J_s = \frac{k_s}{4\pi}P(\mu, \phi; \mu_s, \phi_s)F_s\mu_s e^{-(\tau_e/\mu_s)} \tag{14}$$

where μ_s is the cosine of the solar zenith angle, Φ_s is the solar azimuth and F_s is the solar irradiance. As example, simulations of TOA brightness temperature differences with an without solar contribution show for SEVIRI maximum difference of 15 K at 3.8 microns, 0.05 K at 8.7 microns and 0.02 K at 11 and 12 microns. However, in these simulations the solar contribution increased the calculation time by 40%.

5   Conclusion and perspectives

For more than 30 years, fast RTMs have been developed and maintained for operational assimilation in NWP model. This is possible thanks to the fast calculation of the atmospheric transmittance based on predictors. Nowadays, the two most widely used RTM – RTTOV and CRTM – have proven their efficiency to assimilate radiances in clear-sky and overcast conditions in the infrared and in all-sky conditions in microwave. They also have already implemented new capabilities not currently used in satellite data assimilation (IR cloud scattering scheme, NLTE effect, solar contribution) and many others that were not described in this paper (lambertian surface, aerosol and VIS/NIR simulations). Many issues still remain and new developments are still needed. Those include improvements in spectroscopic databases that are at the heart of RTMs and are being continuously updated for coefficient calculations. These includes also improvements in cloud optical properties modelization and parameterization as well as the treatment of the cloud overlapping especially in the infrared band.

The necessity to implement SO_2 as an active gas is also a new feature that will help the assimilation and prediction of volcanic plumes. As a last step of the job the validation exercise of new version is a important step to provide accuracy of RTM model. These have to be in both clear and cloudy sky.

In near future (2020 and beyond) with the launch of new instruments like IASI-NG (2 times more channels with better SNR) or MTG-IRS (hyperspectral sounder on geostationary satellite with hourly observations), faster satellite data assimilation is already needed. New techniques are already developed. The most advanced one is the use of reconstructed spectra based on principal component. RTM already exist like PC-RTTOV and preliminary test are already encouraging. For example, Matricardi and McNally (2014) have shown a 25% reduction in the overall cost of assimilation with marginal improvement when assimilated 20 PCs against 165 IASI channels. Another promising techniques that are still not at the stage of assimilation exercise is the use of optimal sampling of absorption coefficients like the OSS model (Moncet et al., 2003). This techniques is particularly interesting because it should be better to handle scattering than in current fast RTM.

References

Aires, F., Prigent, C., Bernardo, F., Jiménez, C., Saunders, R., and Brunel, P., 2011: A Tool to Estimate Land-Surface Emissivities at Microwave frequencies (TELSEM) for use in numerical weather prediction. *Q. J. R. Meteorol. Soc.*, **137**, 690– 699, doi: 10.1002/qj.803.

Bauer, P., Moreau, E., Chevallier, F. and O'keeffe, U., 2006: Multiple-scattering microwave radiative transfer for data assimilation applications. *Q. J. R. Meteorol. Soc.*, **132**, 1259–1281, doi: 10.1256/qj.05.153.

Borbas, E., and Ruston, B. C., 2010: The RTTOV UWiremis IR land surface emissivity module, Report NWPSAF-MO-VS-04. *EUMETSAT Associate Visiting Mission Report*, Available at http://nwpsaf.eu/vs_reports/nwpsaf-mo-vs-042.pdf.

Cao, C., Xu, H., Sullivan, J., McMillin, L., Ciren, P., and Hou, Y.-T., 2005: Intersatellite Radiance Biases for the High-Resolution Infrared Radiation Sounders (HIRS) on board NOAA-15, -16, and -17 from Simultaneous Nadir Observations. *J. Atmos. Oceanic Technol.*, **22**, 381–395, doi:10.1175/JTECH1713.1.

Chahine, M. T., 1974: Remote Sounding of Cloudy Atmospheres. I. The Single Cloud Layer. *J. Atmos. Sci.*, **31**, 233–243, doi:10.1175/1520-0469(1974)031<0233:RSOCAI>2.0.CO;2.

Chen, Y., Weng, F., Han, Y., and Liu, Q., 2008: Validation of the Community Radiative Transfer Model by using CloudSat data. *J. Geophys. Res.*, **113**, D00A03, doi:10.1029/2007JD009561.

Chen, Y., Han, Y., Van Delst, P., and Weng, F., 2010: On water vapor Jacobian in fast radiative transfer model. *J. Geophys. Res.*, **115**, D12303, doi:10.1029/2009JD013379.

Chen, Y., Han, Y., van Delst, P., and Weng, F., 2013: Assessment of Shortwave Infrared Sea Surface Reflection and Nonlocal Thermodynamic Equilibrium Effects in the Community Radiative Transfer Model Using IASI Data. *J. Atmos. Oceanic Technol.*, **30**, 2152–2160, doi:10.1175/JTECH-D-12-00267.1.

Chevallier, F., Di Michele, S., and McNally, A. P., 2006: Diverse profile datasets from the ECMWF 91-level short-range forecasts. *NWP SAF Document*, NWPSAF-EC-TR-010, 16 pp.

Chou, M.-D., Lee, K.-T., Tsay, S.-C., and Fu, Q., 1999: Parameterization for Cloud Longwave Scattering for Use in Atmospheric Models. *J. Climate*, **12**, 159–169.

Collard, A. D., 2007: Selection of IASI channels for use in numerical weather prediction. *Q.J.R. Meteorol. Soc.*, **133**, 1977–1991, doi:10.1002/qj.178.

Doppler, L., Preusker, R., Bennartz R., and Fischer, J., 2014: k-bin and k-IR: k-distribution methods without correlation approximation for non-fixed instrument response function and extension to the thermal infrared—Applica tions to satellite remote sensing. *J. Quant. Spectrosc. Radiat. Transfer*, **133**, 382–395, doi:10.1016/j.jqsrt.2013.09.001.

Eyre, J. R., 1991: A fast radiative transfer model for satellite sounding systems. *ECMWF Tech. Memo. No. 176*, Available at http://old.ecmwf.int/publications/library/ecpublications/_pdf/tm/001-300/tm176.pdf.

Field, P. R., Heymsfield, A. J., and Bansemer, A., 2007: Snow Size Distribution Parameterization for Midlatitude and Tropical Ice Clouds. *J. Atmos. Sci.*, **64**, 4346–4365, doi:10.1175/2007JAS2344.1.

Garand, L., et al., 2001: Radiance and Jacobian intercomparison of radiative transfer models applied to HIRS and AMSU channels. *J. Geophys. Res.*, **106**, 24017–24031, doi:10.1029/2000JD000184.

Geer, A. J., Bauer, P., and O'Dell, C. W., 2009: A Revised Cloud Overlap Scheme for Fast Microwave Radiative Transfer in Rain and Cloud. *J. Appl. Meteorol. Climatol.*, **48**, 2257–2270, doi:10.1175/2009JAMC2170.1.

Geer, A. J., and Baordo, F., 2014: Improved scattering radiative transfer for frozen hydrometeors at microwave frequencies. *Atmos. Meas. Tech. Discuss.*,**7**, 1749-1805, doi:10.5194/amtd-7-1749-2014.

Han, Y., and Weng, F., 2006: A fast radiative transfer model for SSMIS upper air sounding channels affected by Zeeman splitting and its application for temperature retrieval. *Proc. 15th Int. TOVS Study Conf.*

Heidinger, A. K., O'Dell, C. W., Bennartz, R., and Greenwald, T., 2006: The Successive-Order-of-Interaction Radiative Transfer Model. Part I: Model Development. *J. Appl. Meteorol. Climatol.*, **45**, 1388–1402, doi:10.1175/JAM2387.1.

Jacquinet-Husson, N., and 52 coauthors, 2008: The GEISA spectroscopic database: Current and future archive for Earth and planetary atmosphere studies. *J. Quant. Spectrosc. Radiat. Transfer*, **109**, 1043-1059, doi:10.1016/j.jqsrt.2007.12.015.

Karbou, F., Prigent, C., Eymard, L. and Pardo, J., 2005: Microwave land emissivity calculations using AMSU-A and AMSU-B measurements. *IEEE Trans. Geosci. Remote Sensing*, **43**, 948–959.

Kobayashi, S., Matricardi, M., Dee, D. and Uppala, S., 2009: Toward a consistent reanalysis of the upper stratosphere based on radiance measurements from SSU and AMSU-A. *Q. J. R. Meteorol. Soc.*, **135**, 2086–2099, doi: 10.1002/qj.514.

Liu, G., 2008: A database of microwave single-scattering properties for nonspherical ice particles. *Bull. Am. Meteorol. Soc.*, **111**, 1563–1570, doi:10.1175/2008BAMS2486.1.

Liu, Q., Weng, F., and English, S. J., 2011: An Improved Fast Microwave Water Emissivity Model. *IEEE Trans. Geosci. Remote Sensing*, **49**, 1238–1250, doi: 10.1109/TGRS.2010.2064779.

Liu, Q., and Weng, F., 2013: Using Advanced Matrix Operator (AMOM) in Community Radiative Transfer Model. *IEEE J. Selected Topics in Applied Earth Observations and Remote Sensing*, **6**, 1211–1218, doi: 10.1109/JSTARS.2013.2247026.

Lu, Q., and Bell, W., 2014: Characterizing Channel Center Frequencies in AMSU-A and MSU Microwave Sounding Instruments. *J. Atmos. Oceanic Technol.*, **31**, 1713–1732, doi: 10.1175/JTECH-D-13-00136.1

Martinet, P., Fourrié, N., Bouteloup, Y., Bazile, E. and Rabier, F., 2014a: Toward the improvement of short-range forecasts by the analysis of cloud variables from IASI radiances. *Atmos. Sci. Lett.*, doi: 10.1002/asl2.510.

Martinet, P., Lavanant, L., Fourrié, N., Rabier, F.and Gambacorta, A., 2014b: Evaluation of a revised IASI channel selection for cloudy retrievals with a focus on the Mediterranean basin. *Q. J. R. Meteorol. Soc.*, **140**, 1563–1577, doi: 10.1002/qj.2239.

Matricardi, M., Chevallier, F., Kelly, G., and Thépaut, J.-N., 2004: An improved general fast radiative transfer model for the assimilation of radiance observations. *Q. J. R. Meteorol. Soc.*, **130**, 153–173, doi: 10.1256/qj.02.181.

Matricardi, M., 2005: The inclusion of aerosols and clouds in RTIASI, the ECMWF fast radiative transfer model for the infrared atmospheric sounding interferometer. *ECMWF Tech. Memo. No. 474.*

Matricardi, M., 2009: Technical Note: An assessment of the accuracy of the RTTOV fast radiative transfer model using IASI data. *Atmos. Chem. Phys.*, **9**, 6899-6913, doi:10.5194/acp-9-6899-2009.

Matricardi, M. and McNally, A. P., 2014: The direct assimilation of principal components of IASI spectra in the ECMWF 4D-Var. *Q. J. R. Meteorol. Soc.*, **140**, 573–582, doi:10.1002/qj.2156.

McMillin, L. M., and Fleming H. E., 1976: Atmospheric transmittance of an absorbing gas: a computationally fast and accurate transmittance model for absorbing gases with constant mixing ratios in inhomogeneous atmospheres. *Appl. Opt.*, **15**, 358–363.

McMillin, L. M., Fleming, H. E., and Hill, M. L., 1979: Atmospheric transmittance of an absorbing gas. 3: A computationally fast and accurate transmittance model for absorbing gases with variable mixing ratios. *Appl. Opt.*, **18**, 1600–1606.

McMillin, L. M., Xiong, X., Han, Y., Kleespies, T. J., and Van Delst, P., 2006: Atmospheric transmittance of an absorbing gas. 7. Further improvements to the OPTRAN 6 approach. *Appl. Opt.*, **45**, 2028–2034.

McNally, A. P., 2009: The direct assimilation of cloud-affected satellite infrared radiances in the ECMWF 4D-Var. *Q. J. R.Meteorol. Soc.*, **135**, 1214–1229, doi: 10.1002/qj.426.

Mlawer, E. J., Payne, V. H., Moncet, J.-L., Delamere, J. S., Alvarado, M. J., and Tobin, D. D., 2012: Development and recent evaluation of the MT_CKD model of continuum absorption. *Phil. Trans. Roy. Soc. A*, **370**, 1–37, doi:10.1098:rsta.2011.0295.

Moncet, J.-L., Uymin, G., Lipton, A. E., and Snell, H. E., 2008: Infrared radiance modeling by optimal spectral sampling. *J. Atmos. Sci.*, **65**, 3917–3934.

Pavelin, E. G., English, S. J., and Eyre, J. R., 2008: The assimilation of cloud-affected infrared satellite radiances for numerical weather prediction. *Q. J. R. Meteorol. Soc.*, **134**, 737–749, doi: 10.1002/qj.243.

Petty, G.W., 2006: *A First Course in Atmospheric Radiation* (2nd. Ed.), Sundog Publishing, 460 pp.

Rothman, L. S., and 42 coauthors, 2009: The HITRAN 2008 molecular spectroscopic database. *J. Quant. Spectrosc. Radiat. Transfer*, **110**, 533-572, doi: 10.1016/j.jqsrt.2009.02.013.

Saunders, R., Matricardi, M. and Brunel, P., 1999: An improved fast radiative transfer model for assimilation of satellite radiance observations. *Q. J. R. Meteorol. Soc.*, **125**, 1407–1425, doi: 10.1002/qj.1999.49712555615.

Saunders, R., et al., 2007: A comparison of radiative transfer models for simulating Atmospheric Infrared Sounder (AIRS) radiances. *J. Geophys. Res.*, **112**, D01S90, doi:10.1029/2006JD007088.

Sherlock, V., 1999: ISEM-6: Infrared Surface Emissivity Model for RTTOV-6. *Met Office NWP SAF Rep.*, **299**, 17 pp.

Strow, L. L., Hannon, S. E., De Souza-Machado, S., Motteler, H.E., and Tobin, D., 2003: An overview of the AIRS radiative transfer model. *IEEE Trans. Geosci. Remote Sensing*, **41**, 303–313, doi: 10.1109/TGRS.2002.808244.

Tobin, D. C., Revercomb, H. E., Moeller, C. C., and Pagano, T. S., 2006: Use of Atmospheric Infrared Sounder high–spectral resolution spectra to assess the calibration of Moderate resolution Imaging Spectroradiometer on EOS Aqua. *J. Geophys. Res.*, **111**, D09S05, doi:10.1029/2005JD006095.